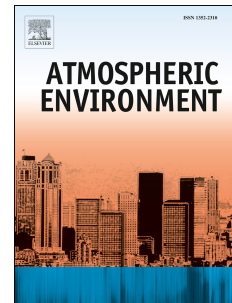


Accepted Manuscript

Using a gradient boosting model to improve the performance of low-cost aerosol monitors in a dense, heterogeneous urban environment

Nicholas E. Johnson, Bartosz Bonczak, Constantine E. Kontokosta



PII: S1352-2310(18)30250-4

DOI: [10.1016/j.atmosenv.2018.04.019](https://doi.org/10.1016/j.atmosenv.2018.04.019)

Reference: AEA 15952

To appear in: *Atmospheric Environment*

Received Date: 21 August 2017

Revised Date: 9 April 2018

Accepted Date: 10 April 2018

Please cite this article as: Johnson, N.E., Bonczak, B., Kontokosta, C.E., Using a gradient boosting model to improve the performance of low-cost aerosol monitors in a dense, heterogeneous urban environment, *Atmospheric Environment* (2018), doi: 10.1016/j.atmosenv.2018.04.019.

This is a PDF file of an unedited manuscript that has been accepted for publication. As a service to our customers we are providing this early version of the manuscript. The manuscript will undergo copyediting, typesetting, and review of the resulting proof before it is published in its final form. Please note that during the production process errors may be discovered which could affect the content, and all legal disclaimers that apply to the journal pertain.

Using a gradient boosting model to improve the performance of low-cost aerosol monitors in a dense, heterogeneous urban environment

Nicholas E. Johnson^{a,b}, Bartosz Bonczak^b, Constantine E. Kontokosta*^b

^a*University of Warwick, United Kingdom*

^b*New York University, United States*

*corresponding author: ckontokosta@nyu.edu

Abstract

The increased availability and improved quality of new sensing technologies have catalyzed a growing body of research to evaluate and leverage these tools in order to quantify and describe urban environments. Air quality, in particular, has received greater attention because of the well-established links to serious respiratory illnesses and the unprecedented levels of air pollution in developed and developing countries and cities around the world. Though numerous laboratory and field evaluation studies have begun to explore the use and potential of low-cost air quality monitoring devices, the performance and stability of these tools has not been adequately evaluated in complex urban environments, and further research is needed. In this study, we present the design of a low-cost air quality monitoring platform based on the Shinyei PPD42 aerosol monitor and examine the suitability of the sensor for deployment in a dense heterogeneous urban environment. We assess the sensor's performance during a field calibration campaign from February 7th to March 25th 2017 with a reference instrument in New York City, and present a novel calibration approach using a machine learning method that incorporates publicly available meteorological data in order to improve overall sensor performance. We find that while the PPD42 performs well in relation to the reference instrument using linear regression ($R^2=0.36-0.51$), a gradient boosting regression tree model can significantly improve device calibration ($R^2=0.68-0.76$). We discuss the sensor's performance and reliability when deployed in a dense, heterogeneous urban environment during a period of significant variation in weather conditions, and important considerations when using machine learning techniques to improve the performance of low-cost air quality monitors.

Keywords: Machine learning, Low-cost sensing, Air quality, Urban, Calibration

1. Introduction

Air quality is an important quality of life concern with well-established links to serious respiratory illnesses, cardiovascular disease, and increased mortality rates (Pope III and Dockery, 2006). Cities in particular often experience high levels of fine particulate matter (PM2.5), especially in developing countries where industrial expansion has created unprecedented levels of poor air quality (Cheng et al., 2016). In order to monitor and evaluate levels of PM2.5, government agencies often operate air quality monitoring stations that provide ambient PM2.5 concentration measurements. These networks, however, often fail to capture the granular spatiotemporal variations in PM2.5 levels that can occur over short distances (<1km) (Castell et al., 2017). Urban environments, in particular, contain widely varying mixing ratios with diverse and complex emission

sources that require high resolution spatial and temporal monitoring networks to adequately quantify and describe air quality (Mead et al., 2013).

The proliferation of low-cost sensor technologies offers new opportunities to monitor and study air quality in urban environments. A growing body of research has begun to use low-cost aerosol monitors to provide high resolution spatiotemporal measurements by creating dense spatial networks that can inform local and regional emission sources' contribution to total pollution levels, as well as increase the ability to identify pollution hot-spots (Heimann et al., 2015; Jerrett et al., 2005; Shusterman et al., 2016; Manikonda et al., 2016; Moltchanov et al., 2015). Furthermore, these low-cost technologies are often compact, low-powered, and easy to operate, thus offering the ability to establish and facilitate participatory networks (Jovašević-Stojanović et al., 2015; Snyder et al., 2013). High density air qual-

36 ity monitoring networks enable community-based feed-
 37 back loops that can be used to both protect those indi-
 38 viduals susceptible to poor air quality and identify spe-
 39 cific causes of particulate matter pollution.

40 While low-cost devices offer new opportunities for
 41 large-scale air quality monitoring, there are several im-
 42 portant limitations to be considered. Central to the is-
 43 sue of using low-cost devices is ensuring data quality
 44 (Snyder et al., 2013; Kumar et al., 2015). Though fed-
 45 eral, state and local monitoring devices operate at sig-
 46 nificantly higher costs, they also operate under stand-
 47 ard procedures for calibration, data collection, and
 48 data post-processing methods, which ensure consist-
 49 ency across devices. In contrast, low-cost devices often
 50 suffer from a lack of manufacturer information about the
 51 specific operation and limitations of the device, as well
 52 as employ simplistic sampling techniques that funda-
 53 mentally inhibit the device's performance ability. Fur-
 54 thermore, low-cost sensors often require individual and
 55 frequent calibration, which involves regular access to
 56 expensive equipment and expertise, and can be imprac-
 57 tical for a large-scale deployments. To address many
 58 of these challenges, a number of studies have eval-
 59 uated multivariate calibration using machine learning
 60 techniques (De Vito et al., 2018; Fishbain and Moreno-
 61 Centeno, 2016).

62 In this study, we present the design of a low-cost
 63 air quality monitoring platform based on the Shinyei
 64 PPD42 aerosol monitor and examine the suitability of
 65 the sensor for deployment in a dense spatial network
 66 configuration. We assess the sensor's performance dur-
 67 ing a field calibration campaign from February 7th to
 68 March 25th 2017 with a reference instrument in New
 69 York City and present a novel calibration approach us-
 70 ing a machine learning method that incorporates pub-
 71 licly available meteorological data in order to improve
 72 the sensor's performance.

73 This work is a part of a long-term study, the *Quan-*
 74 *tified Community*, aimed to understand neighborhoood-
 75 scale interactions between the environment and man-
 76 made infrastructure and their effects on individuals and
 77 communities Kontokosta (2016). To understand this
 78 complex interaction, we aim to leverage low-cost tech-
 79 nologies to create a dense sensor network in neighbor-
 80 hoods throughout New York City that provides real-time
 81 and granular spatiotemporal environmental data. The
 82 air quality monitoring platform described in this work is
 83 one aspect of a multi-sensor platform being developed.

84 2. Materials and Methods

85 2.1. Node Design

86 The *Quantified Community* sensor platform was de-
 87 veloped using commodity hardware and designed to
 88 capture environmental parameters including fine partic-
 89 ultate mater, ambient noise level, air temperature, rela-
 90 tive humidity and luminosity. To achieve a high den-
 91 sity monitoring network, the selection of sensors and
 92 platform hardware required careful consideration in or-
 93 der to find a balance between performance, reliability,
 94 accuracy, cost and scalability. Our sensor platform is
 95 designed to be deployed in a variety of urban environ-
 96 ments, including dense, high-rise neighborhoods with
 97 comprehensive digital infrastructure to low density, eco-
 98 nomically disadvantaged communities with incomplete
 99 access to power and wireless network connectivity.

100 The Shinyei PPD42 was selected to measure PM_{2.5}
 101 because of its low cost, ease of use, and performance ca-
 102 pability demonstrated in previous work (Holstius et al.,
 103 2014; Gao et al., 2015; Kelly et al., 2017; Austin et al.,
 104 2015; Jovašević-Stojanović et al., 2015; Wang et al.,
 105 2015). The PPD42 uses a light scattering technique to
 106 estimate particle concentration and is capable of mea-
 107 suring particles greater than 1 μm in diameter. Particles
 108 pass through a lighting chamber where the combination
 109 of a light emitter and photodiode detector measure the
 110 amount of light scattered by particles passing through
 111 the chamber. A 0.25W thermal resistor, located at the
 112 bottom of the sensing chamber, increases the air tem-
 113 perature inside the chamber relative to the surrounding
 114 outside air temperature to create an updraft that draws
 115 particles into and through the chamber.

116 The PPD42 generates two output signals in the form
 117 of digital pulses that are referred to by the manufacturer
 118 as Low Pulse Occupancy (LPO) and are proportional to
 119 particle count concentration. In order to distinguish par-
 120 ticle size, output P1 is used to measure particles greater
 121 than 1 μm and output P2 is used to measure particles
 122 greater than 2.5 μm . Particles with a diameter between
 123 1 μm and 2.5 μm are determined by subtracting P2 from
 124 P1. The PPD42 outputs are connected to the interrupt
 125 pints (INT0 and INT1) of an Atmega microcontroller in
 126 order to accurately capture pulses that range from 10-90
 127 milliseconds in length. The raw sensor output is con-
 128 verted into LPO readings and sent to a Raspberry Pi
 129 microcontroller via USB every 10 seconds to be stored
 130 locally. Though the Raspberry Pi is capable of transmit-
 131 ting the data to a central server for real-time processing,
 132 there was no available Wi-Fi connectivity in the study
 133 area.

134 A factory calibrated Bosch SHT31 sensor was used
 135 to measure air temperature and relative humidity with
 136 an accuracy of $\pm 0.3^{\circ}\text{C}$ and $\pm 2\%$ relative humidity. The
 137 electronics were contained in a 6"x4"X2" gray ABS
 138 plastic enclosure with a 5VDC fan attached to the bot-
 139 tom in order to draw air into the enclosure through a 1
 140 1/2" filtered vent. Based on the manufacturer specifi-
 141 cations, we estimate complete air exchange inside the
 142 enclosure occurs approximately three times per second.

143 The PPD42 sensor used in this study cost approx-
 144 imately \$15USD. Additional sensors, the microcon-
 145 troller platform, and enclosure materials added an ad-
 146 ditional \$80 USD resulting in an overall cost of approx-
 147 imately \$100 USD, which is several orders of magni-
 148 tude less than reference instruments operated by state
 149 and federal agencies.

150 2.2. Reference Instrument

151 The reference instrument for this study was a Thermo
 152 Scientific tapered element oscillating microbalance
 153 (TEOM) 1400 that provides continuous PM2.5 mass
 154 measurements at hourly intervals. TEOM instruments
 155 employ a size selective inlet that accumulates particles
 156 on a sampling filter located atop of an oscillating ele-
 157 ment whose resonant frequency changes proportionally
 158 to particle mass (Kulkarni et al., 2011; Amaral et al.,
 159 2015). The device is owned and operated by the New
 160 York State Department of Environmental Conservation
 161 (NYS DEC) and costs approximately \$30,000. Data
 162 from the reference instrument were obtained directly
 163 from the Department of Environmental Conservation¹.
 164 It was observed that the data contained 32 observations
 165 with negative values due to the processing procedure
 166 performed by the NYS DEC; these measurements were
 167 subsequently removed from the analysis.

168 2.3. Study Location

169 The study site was located at an elementary school
 170 (PS 104) rooftop on Division Street in Lower Manhat-
 171 tan. The location is a dense urban area with varying in-
 172 frastructure comprised of approximately 11% commer-
 173 cial buildings, 10% residential buildings, 22% mixed
 174 residential and commercial and 2% industrial buildings
 175 within 1000m, based on information from NYC's Pri-
 176 mary Land Use Tax Output (PLUTO) database. Ta-
 177 ble S3 provides a description of the surrounding char-
 178 acteristics. Of important note, the site is located less
 179 than 50 meters from the Manhattan Bridge with an
 180 average of 115,000 vehicles crossing every day (New

181 York State Department of Transportation, 2017). The
 182 study area also contains approximately 56 buildings that
 183 use oil boiler systems, which are known to be signif-
 184 icant sources of particulate matter in New York City
 185 (Clougherty et al., 2013).

186 The individual nodes were fixed on a custom mount-
 187 ing platform at a height of approximately 1.5m above
 188 the rooftop (approximately 12m from ground level) and
 189 3m from the rooftop edge. The design of the mounting
 190 platform positioned two devices facing east towards the
 191 Manhattan bridge and one device facing west away from
 192 the bridge. The devices were located approximately 5m
 193 from the intake of the reference instrument due to logis-
 194 tical reasons.

195 2.4. PPD42 Performance Evaluation

196 An initial evaluation of the PPD42 was conducted to
 197 assess the accuracy and precision of the three individ-
 198 ual deployed devices. Raw LPO readings were aggre-
 199 gated to an hourly average in order to match data from
 200 the reference monitor, and pairwise plots were used to
 201 compare individual sensor responses with the reference
 202 monitor. To evaluate the linear relationship between
 203 individual devices and the reference monitor, an Ordin-
 204 ary Least Squares (OLS) regression was performed on
 205 the matched hourly data and the coefficient of deter-
 206 mination (R^2) and the root mean squared error (RMSE)
 207 values were used to evaluate the strength and accuracy
 208 of the relationship. In this study, measurements from
 209 the TEOM monitor are used as the dependent variable
 210 and measurements from the PPD42 are the independent
 211 variable.

212 A sensitivity analysis was performed using multiple
 213 meteorological parameters to determine their potential
 214 influence on sensor measurements. The coefficient of
 215 determination was used to evaluate the strength of the
 216 relationship between meteorological parameters (inde-
 217 pendent variables) and the PPD42 and TEOM mea-
 218 surements (dependent variables). Temperature and humidity
 219 measurements were taken directly from individual sen-
 220 sor platforms using the SHT31 sensor located inside the
 221 enclosure directly adjacent to the PPD42. Other meteo-
 222 rological parameters were also assessed including baro-
 223 metric pressure, wind speed, dew point, and precipitation.
 224 These measurements were obtained from a nearby
 225 weather station located at La Guardia airport. Figure
 226 1 shows the meteorological conditions during the study
 227 period.

228 In order to determine the device's sensitivity in low
 229 concentration environments, the lower limit of detection
 230 was calculated as:

¹www.dec.ny.gov

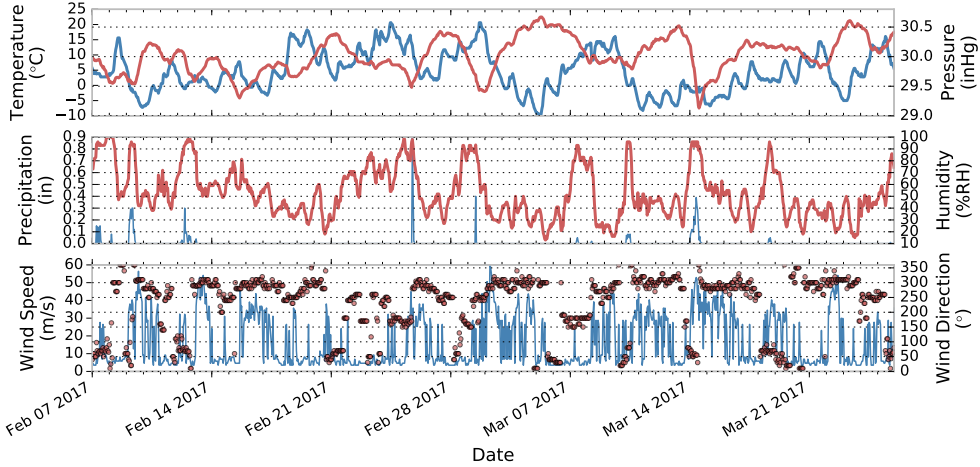


Figure 1: Meteorological measurements taken from La Guardia airport over the study period. (a) Temperature (blue) and sea level pressure (red), (b) precipitation (blue) and humidity (red line), and (c) wind speed (blue line) and wind direction (red points).

$$LOD = 3\sigma_{blk} * \beta_1$$

where σ_{blk} is the standard deviation of the PPD42 measurements obtained when TEOM measurements were below $5.0\mu\text{g}/\text{m}^3$, $3.0\mu\text{g}/\text{m}^3$ and $1.0\mu\text{g}/\text{m}^3$, and β_1 is the slope of the line obtained from the OLS regression analysis. We include multiple calculations of the LOD in order to provide statistically significant results given the small number of samples from the TEOM below $1.0\mu\text{g}/\text{m}^3$ (14 samples). This approach was established by Kaiser and Specker (1956) and also used in similar studies (Austin et al., 2015; Wang et al., 2015; Kelly et al., 2017).

2.5. Calibration Approaches

Three statistical approaches were evaluated to determine the best-fit calibration model. All three models were based on measurements from the individual sensor platforms, as well as meteorological data that included air temperature, relative humidity, barometric pressure, dew point, and precipitation. As noted in previous work, the PPD42's response is non-linear across the entire range of the device and therefore a quadratic term was also included into the model (Gao et al., 2015; Austin et al., 2015; Wang et al., 2015). A final parameter was added to account for the time of day based on an analysis of diurnal readings from the PPD42 devices, which showed a 1.5 standard deviation difference between the reference instrument during the afternoon hours from 10:00-15:00 (Figure S1). This difference is likely caused by solar radiation affecting the sensor's optics and the inclusion of a time parameter is intended

to capture this phenomenon. R^2 and RMSE were used to compare calibration accuracy.

The first calibration method used a standard multiple linear regression model in the form of:

$$y = \beta_0 + \beta_1 x_1 + \beta_2 x_2 + \dots + \beta_p x_p + \epsilon$$

where y is the reference instrument values, β_0 is the intercept, $x_1 \dots x_p$ are the predictors including the PPD42 measurements, and ϵ is the error term. The model was specified using best-subset selection, which iteratively finds the combination of features that result in the greatest reduction in the residual sum of squares for each subset of size k where $k = p - 1 \dots p$. The single best model from $M_0 \dots M_k$ was chosen based on Bayesian Information Criterion scores. To detect and account for multicollinearity between variables, the variance inflation factor (VIF) was calculated for all features, and the feature with the highest score was removed. This process was performed recursively until all features' VIF scores were below the threshold of five. The final model included only statistically significant features.

The second calibration technique used a regularization method to address some of the problems with least squares regression. Regularization adds a penalty term (λ) to large model coefficients in order to reduce multicollinearity between features. The ridge regression model used here applies an ℓ_2 penalty to the sum of the squared coefficients. Ridge coefficients ($\hat{\beta}^R$) are values that minimize:

$$\sum_{i=1}^n \left(y_i - \beta_0 - \sum_{j=1}^p \beta_j x_{ij} \right)^2 + \lambda \sum_{j=1}^p \beta_j^2$$

where λ controls the amount of penalization. The λ parameter was determined through a five-fold cross validation and set to 0.4. In order to evaluate the significance of individual features, we rank each feature based on the absolute value of the coefficient (β_j). The larger the coefficient, the larger the impact on the model and hence the greater significance of the feature.

The final calibration approach used a gradient boosting regression tree (GBRT) model. GBRT is a decision tree-based regression model that implements boosting to improve model performance. Boosting is a statistical technique that sequentially builds many 'weak' models (learners) that are combined into a final consensus model (Schapire, 2003). A 'weak' learner is one whose performance is only slightly better than random guessing. The final model is built in an additive forward stagewise manner where at each step a new learner is added that minimizes the negative gradient by least squares. The residuals of the current model are then used as the input for the next tree allowing the model to 'learn' from the errors of the previous models (Friedman et al., 2001).

Parameter tuning is an important element to optimize the GBRT model performance. Tree-specific parameters include the depth of each tree, the minimum number of samples to form a terminal node (leaf), and the maximum number of features included in each tree. Boosting parameters include the number of trees used in the model and the contribution of each tree to the final model (learning rate). Tree depth, the number of trees, and the maximum number of features in each tree control the degree of interaction between features. Since trees are grown sequentially, a large number of shallow trees are preferred in order to fully explore the feature space, at the expense of computation time. The learning rate and the minimum number of samples per leaf are used to control overfitting. A low learning rate is generally preferred, but will require a larger number of trees to maintain performance.

To build the ridge and GBRT models, data were first randomly split into train (80%) and test (20%) sets. The training set was used to evaluate model parameters through an exhaustive grid search with 5-fold cross-validation and the final model was evaluated on the test set. All three models were implemented using the scikit-learn package for Python (Pedregosa et al., 2011).

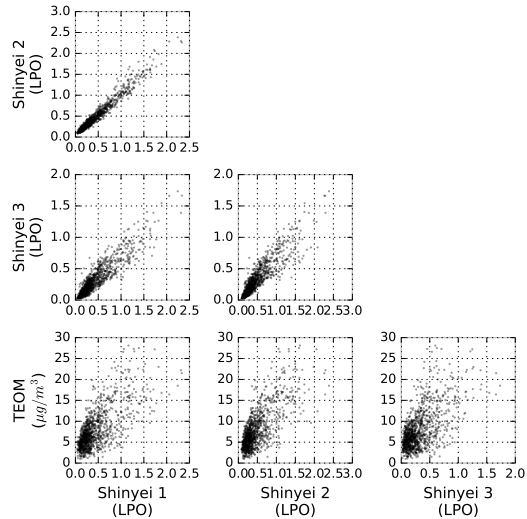


Figure 2: Pairwise plots between three Shinyei PPD42 devices and a reference TEOM based on hourly data collected from February 7th to March 25th 2017.

3. Results and Discussion

All three platform nodes collected data continuously throughout the 47-day study period with the exception of four days in which all three devices experienced a power outage. Figure 2 shows pairwise plots from the co-located PPD42 devices. A total of 1128 hourly observations were recorded from all three devices. Hourly PM2.5 measurements from the TEOM ranged from 1 $\mu\text{g}/\text{m}^3$ to 28.1 $\mu\text{g}/\text{m}^3$ with an average of 7.8 $\mu\text{g}/\text{m}^3$.

Figure 3 shows a scatter plot of the linear fit model between the TEOM and PPD42 devices. Based on the calculated R² values from a linear model fit, individual PPD42 devices demonstrate a moderate level of agreement compared to the TEOM with R² values of 0.48 and 0.53 for two devices and the third device slightly lower at 0.37. These results are similar to previous work by Holstius et al. (2014) who conducted an eight-day field calibration campaign at a regulatory site in Oakland, California and found that a linear correlation was sufficient to explain 55-60% of the variance (RMSE=3.4-3.6) in the federal equivalent method instrument at a one hour interval and 72% at a 24 hour interval. Kelly et al. (2017) also found moderate correlation (R²=0.59-0.8) between the PPD42 and a commercial grade optical device (TSI DustTrak II Model 8532) during ambient wind tunnel tests, and Gao et al. (2015) found similar correlations (R²=0.53) with 24h gravimetric measurements during a four-day calibration campaign in Xi'an, China. Gao et al. (2015), however, also observed signif-

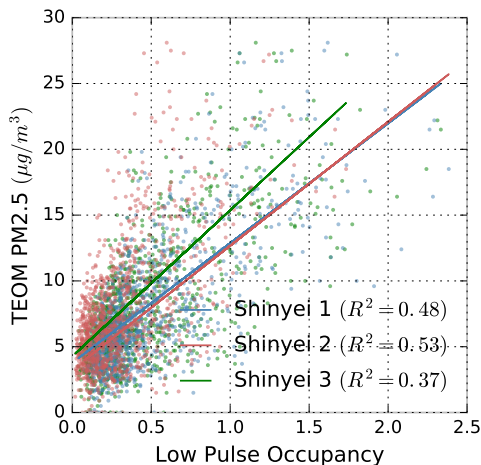


Figure 3: Linear model fit for hourly data collected from three Shinyei PPD42 sensors and a NYS DEC reference monitor between February 7th 2017 and March 25th, 2017.

363 significantly higher hourly correlations ($R^2=0.87-0.88$) with
364 the DustTrak instrument and suggest the higher corre-
365 lation is likely due to the increased levels of PM2.5
366 concentrations observed in Xi'an (range: 77-889 $\mu\text{g}/\text{m}^3$)
367 compared to Holstius et al. (2014) (range: 0.3-30 $\mu\text{g}/\text{m}^3$)
368 since the PPD42's measurement errors increase at lower
369 concentration levels.

370 Individual PPD42 devices show high correlation with
371 R^2 values of 0.93-0.96 and a linear response across the
372 concentration range (Figure S3). This high corre-
373 lation between PPD42 devices has been largely consistent
374 across studies by Holstius et al. (2014), Gao et al. (2015)
375 and Kelly et al. (2017), who all report high inter-device
376 correlations ($R^2 > 0.9$) with the exception of one exper-
377 iment by Kelly et al. (2017) reporting a correlation of
378 $R^2=0.72$.

379 3.1. Ambient Conditions

380 The average temperature during the study period was
381 4.5°C (range: -10.0-20.6°C) with an average humidity
382 of 52% (range: 0-100%). Rapid fluctuations in meteo-
383 rological conditions were observed throughout the study
384 period. For example, the average temperature during
385 the week of February 9th-17th was 0.8°C (range: -7.2-
386 8.2°C) and increased significantly to an average temper-
387 ature of 10.7°C (range: 1.7-20.6°C) the following week.
388 Other extreme weather conditions were also observed
389 including 20 days with high winds (>30m/s), three sep-
390 arate snow days with a total accumulation of five inches
391 and two days with freezing rain. The observed ranges
392 in temperature, humidity, and precipitation are signif-

393 icantly greater than those of previous field calibration
394 studies.

395 Table S1 shows the sensitivity test results. Dew point
396 temperature measurements show the highest correlation
397 between both the PPD42 and the TEOM ($R^2 = 0.38$ -
398 0.41 and $R^2 = 0.18$) compared to other meteorological
399 parameters. Temperature and relative humidity are both
400 weakly correlated ($R^2 = 0.24$ -0.25 and $R^2 = 0.13$ -0.19)
401 with the PPD42 measurements, and show only minor
402 influence on the TEOM ($R^2 = 0.15$). Previous work
403 by Holstius et al. (2014) evaluated the affect of tem-
404 perature, relative humidity and light levels on PPD42
405 measurements and found only relative humidity had mi-
406 nor correlation ($R^2 = 0.25$ -0.28). While we observe
407 the affect of relative humidity to be slightly lower and
408 the affect of temperature to be significantly higher than
409 findings by Holstius et al. (2014), it should be noted
410 that the meteorological conditions during the Holstius
411 et al. (2014) study varied significantly from this study
412 with temperatures ranging from 20 to 30°C and relative
413 humidity ranging between 10-60%. Gao et al. (2015)
414 also found that temperature and relative humidity effects
415 were significant, noting the differences in meteorolog-
416 ical conditions between their work and findings by Hol-
417 stius et al. (2014).

418 Differences between these studies may be explained
419 by the convective technique used to create air flow
420 through the sensing chamber. Since the convective flow
421 generated by the resistor is proportional to the surround-
422 ing air temperature, fluctuations in ambient temperature
423 will have a direct effect on the sensor's ability to draw
424 particles through the sensing chamber. As observed in
425 this study, and noted by Gao et al. (2015) and Kelly
426 et al. (2017), cooler ambient temperatures will more sig-
427 nificantly affect the PPD42 measurements than higher
428 ambient temperatures. Furthermore, Kelly et al. (2017)
429 also compare the PPD42 with a similar optical aerosol
430 monitor, the Plantower PMS3003, and suggest that the
431 improved performance of the PMS3003 may be due to
432 the use of a fan to control air flow through the sensing
433 chamber.

434 3.2. Limit of Detection

435 Table 1 shows results for the PPD42's lower limit
436 of detection. The average LOD is 4.83 $\mu\text{g}/\text{m}^3$ for con-
437 centrations below 5.0 $\mu\text{g}/\text{m}^3$ (323 samples), 3.6 $\mu\text{g}/\text{m}^3$
438 for concentrations below 3.0 $\mu\text{g}/\text{m}^3$ (90 samples) and
439 2.8 $\mu\text{g}/\text{m}^3$ for concentrations below 1.0 $\mu\text{g}/\text{m}^3$ (14 sam-
440 ples). These findings are in the range of laboratory tests
441 performed by Austin et al. (2015) (1.0 $\mu\text{g}/\text{m}^3$) and Wang
442 et al. (2015) (4.59 $\mu\text{g}/\text{m}^3$ and 6.44 $\mu\text{g}/\text{m}^3$).

Table 1: Results from calculating the lower limit of detection for the PPD42 during a field calibration campaign with a TEOM reference instrument. Units are in $\mu\text{g}/\text{m}^3$

Concentration	Sample Size	Shinyei 1	Shinyei 2	Shinyei 3	TEOM
< 1 $\mu\text{g}/\text{m}^3$	14	3.34	2.90	2.30	0.79
< 3 $\mu\text{g}/\text{m}^3$	90	3.35	3.30	4.45	2.75
< 5 $\mu\text{g}/\text{m}^3$	323	4.82	4.65	5.12	3.37

443 3.3. Calibration Results

444 Table 2 and Figure 4 compare OLS, Ridge, and
 445 GBRT results from the hourly test data and show that
 446 the GBRT model significantly outperforms both the
 447 OLS and Ridge models with an average R^2 of 0.72.
 448 While it is expected that the more complex model will
 449 outperform other models, there are two observations
 450 that should be highlighted. First, the overall magni-
 451 tude of improvement by the GBRT model is significant,
 452 increasing by approximately 20-30% over the Ridge
 453 model. Second, the GBRT model also reduces the range
 454 of scores between devices from 0.16 points in the Ridge
 455 model to 0.08 points in the GBRT model. This ability
 456 to reduce device variability is a significant enhancement
 457 for relative calibration and large-scale deployments.

458 Figure 5 compares OLS, Ridge and GBRT calibrated
 459 hourly measurements. Overall, the OLS and Ridge
 460 models show similar R^2 values and track well against
 461 the TEOM monitor. However, results from the OLS
 462 and Ridge models periodically under- and over-estimate
 463 TEOM measurements. Significant under-estimates by
 464 the PPD42, for example, are observed on February
 465 11th and February 16-19th, in which the TEOM in-
 466 strument reported higher PM2.5 concentrations during
 467 both periods. Over-estimates are often found during the
 468 evening hours (e.g. Mar 9-12th) and are likely due to
 469 the low PM2.5 concentration levels that fall below the
 470 PPD42's lower limit of detection. The GBRT model,
 471 however, does not demonstrate the same under- and
 472 over-estimates observed in the OLS and Ridge models.

473 Figure S2 compares feature importance between the
 474 ridge model and GBRT model. The most significant
 475 features in the ridge model are the PPD42 output, sea
 476 level pressure and the squared PPD42 sensor output,
 477 while the GBRT model identifies pressure, dew point,
 478 the PPD42 output and the squared PPD42 sensor out-
 479 put. These results also show that the ridge model places
 480 greater weight on only a few parameters, while relative
 481 feature importance is distributed across features in the
 482 GBRT model. This is expected given that the GBRT
 483 model is a more robust model capable of learning com-
 484 plex relationships across a large set of input parameters.

485 In this case, the model is able to better establish the re-
 486 lationship between sensor measurements and meteorolog-
 487 ical conditions to improve the calibration. Table S2
 488 shows the complete OLS model results with computed
 489 significance values for each parameter for comparison.

490 3.4. Main Findings

491 The aim of this study is to examine the viability of
 492 a low-cost air quality platform based on the PPD42
 493 aerosol monitor to measure PM2.5 in a dense urban
 494 environment. Based on an extensive field calibration
 495 campaign, we find the PPD42 performs reasonably well
 496 throughout a variety of environmental conditions and
 497 can be a suitable device for measuring PM2.5, es-
 498 pecially considering the difference in cost from other
 499 commercially-available instruments. The high corre-
 500 lation between PPD42 devices is particularly signifi-
 501 cant for high-density sensor networks that rely on rel-
 502 ative measurements to inform the spatial distribution
 503 and variability of PM2.5 across a study area. Fur-
 504 thermore, while measurement errors increase at lower
 505 PM2.5 concentrations (< 5 $\mu\text{g}/\text{m}^3$), the limit of detec-
 506 tion falls below the range of ambient concentration lev-
 507 els expected in many urban environments. For example,
 508 New York City's average annual PM2.5 concentra-
 509 tion level is 11.55 $\mu\text{g}/\text{m}^3$ with a range of 5.17-26.48 $\mu\text{g}/\text{m}^3$
 510 (Matte et al., 2013).

511 An important consideration in evaluating acceptable
 512 detection limits is the specific application and use of
 513 the recorded particulate matter observations. Larger
 514 measurement errors from low-cost devices may still be
 515 acceptable to compare ambient PM2.5 levels between
 516 communities, identify local hot spots, and provide feed-
 517 back to local residents. Furthermore, the temporal res-
 518 olution offered by many low-cost devices, including the
 519 PPD42, can be useful in measuring transient emission
 520 sources that may significantly exceed ambient concen-
 521 tration levels over short time periods.

522 Through comparing various calibration techniques,
 523 this study found that a GBRT model that uses publicly
 524 available meteorological data can significantly improve
 525 the performance of a low-cost aerosol monitor. While

Table 2: Comparison of results from three calibration techniques.

Parameter	OLS				Ridge				GBRT			
	R^2	RMSE	β_0	Slope	R^2	RMSE	β_0	Slope	R^2	RMSE	β_0	Slope
Shinyei 1	0.452	3.28	3.60	0.59	0.466	3.24	3.35	0.62	0.716	2.36	1.84	0.79
Shinyei 2	0.507	3.11	3.28	0.64	0.521	3.07	2.99	0.67	0.762	2.16	1.47	0.83
Shinyei 3	0.360	3.55	4.74	0.44	0.364	3.54	4.31	0.48	0.678	2.52	2.48	0.72

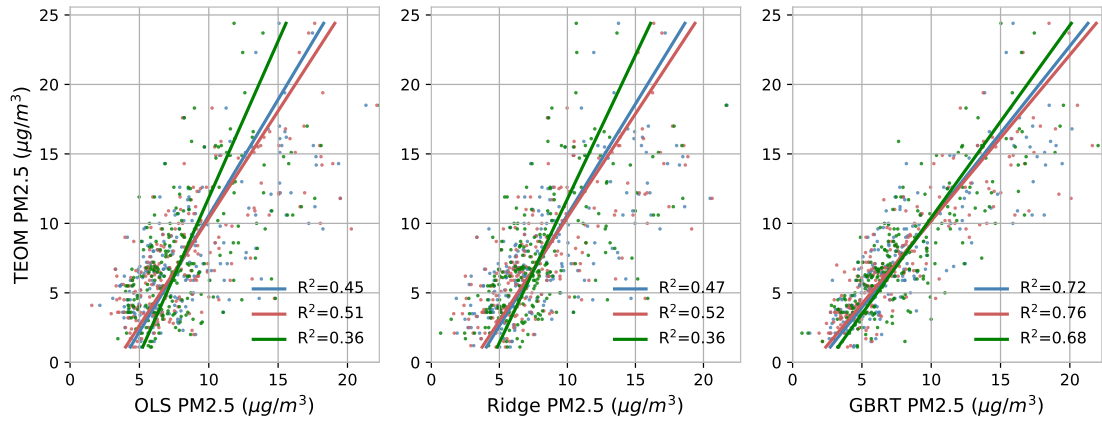


Figure 4: Scatter plots of three Shinyei PPD42 sensors calibrated with three different techniques. Sensors are calibrated through a multi-linear regression, ridge regression and gradient boosting regression tree model.

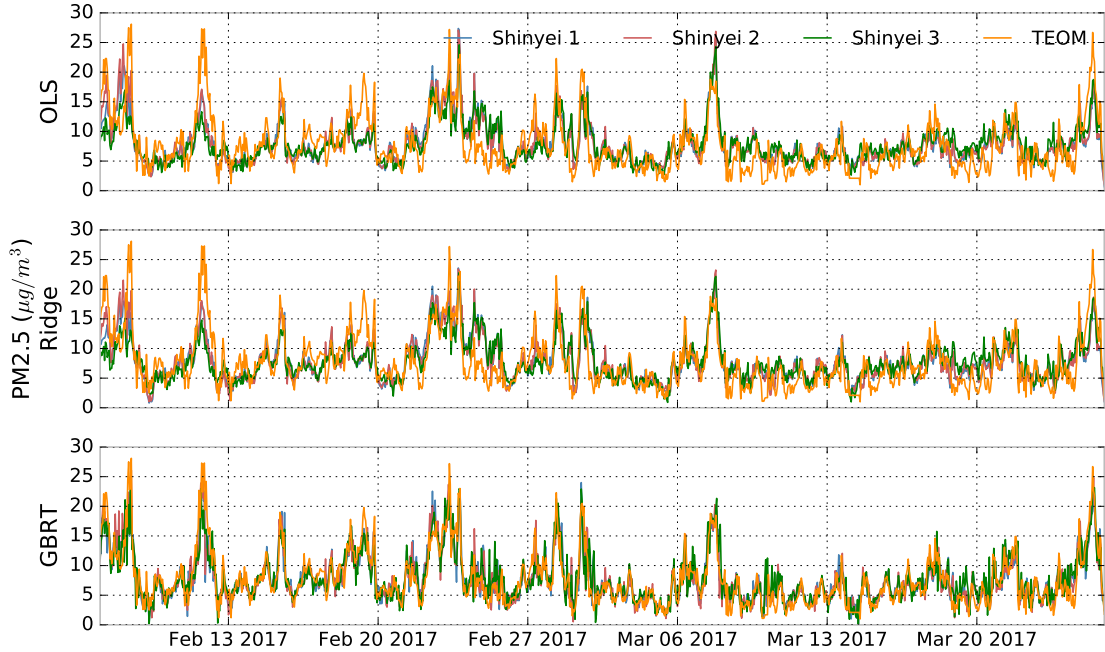


Figure 5: Comparison of calibration results with a reference instrument using different calibration techniques including multiple linear regression, ridge regression and gradient boosting regression tree models. Hourly PM2.5 measurements were obtained from three Shinyei PPD42 sensors co-located with a TEOM reference instrument from February 7th through March 25th, 2017.

526 this calibration process does not necessarily establish 577
 527 an equivalence between the devices, it does provide a 578
 528 method for converting raw sensor readings into standard 579
 529 units ($\mu\text{g}/\text{m}^3$) and improve the sensor's performance by 580
 530 identifying meteorological conditions that cause mea- 581
 531 surement error and adjusting the sensor's response ac- 582
 532 cordingly. Furthermore, the implementation of a ML 583
 533 model to calibrate low-cost instruments can be a step to- 584
 534 wards a universal calibration curve and standardize sen- 585
 535 sor deployments. A properly trained ML model could 586
 536 be publicly distributed and implemented in similar hard- 587
 537 ware deployments by citizen science communities and 588
 538 nonspecialists, which could reduce the need to calibrate 589
 539 devices individually, improve long-term device stability, 590
 540 and standardize data generation and collection methods. 591

541 3.5. Limitations

542 A significant limitation when using the PPD42 is the 594
 543 inability to explain measurement errors and variability 595
 544 between the PPD42 devices. This is largely a result of 596
 545 the optical sensing technique employed. Unlike other 597
 546 sampling techniques, the light scattering approach used 598
 547 by many low-cost aerosol monitors is unable to eval- 599
 548 uate the physical properties of particles such as composi- 600
 549 tion, type, mass, or optical characteristics. For example, 601
 550 organic particles tend to absorb moisture from the sur- 602
 551 rounding environment making them more susceptible to 603
 552 changes in humidity. Similarly, different particle types 604
 553 have different optical properties that can vary depending 605
 554 on the wavelength of light used in the sensor.

555 This work is also limited by the use and compari- 607
 556 son of three sensing units, which limits a full evalua- 608
 557 tion of inter-device variation. Though our analysis is 609
 558 consistent with previous work showing high correlation 610
 559 ($R^2=0.93-0.96$) between PPD42 devices, a more robust 611
 560 statistical analysis that includes greater than 10 devices 612
 561 has yet to be performed. Similarly, while the calibra- 613
 562 tion campaign does provide sufficient data to assess the 614
 563 sensor's performance in concentration ranges typical for 615
 564 New York City, these ranges may vary significantly in 616
 565 other urban areas around the world. To ensure accurate 617
 566 calibration, especially when using ML techniques, the 618
 567 devices should be exposed to the entire range of con- 619
 568 centrations expected during deployment in order to in- 620
 569 clude the training data necessary for the model to es- 621
 570 tablish the proper input-response relationship. Further- 622
 571 more, the study duration also limits an evaluation of 623
 572 long-term stability ($>1\text{yr}$) and time-in-use effects such 624
 573 as the gradual accumulation of particles inside the sens- 625
 574 ing chamber, which may effect the sensor's optics.

575 There are also several important limitations to imple- 626
 576 menting machine learning algorithms for sensor calibra-

577 tion. One significant challenge is the potential to overfit 578 the model to either the specific environment in which 579 the calibration took place, or to the sample data used for 580 the calibration. The latter is a general concern whenever 581 using machine learning models and can be addressed 582 with various techniques such as cross validation, as im- 583 plemented in this analysis. Overfitting the calibration 584 environment, however, can occur by incorporating pa- 585 rameters into the calibration model that are either spe- 586 cific to the calibration location, or do not include the 587 full range of conditions that the sensor will be exposed 588 to during deployment. It is essential that individual pa- 589 rameters contain sufficient variance to properly capture 590 potential deployment conditions, while excluding any 591 spatial parameters that could potentially affect the in- 592 put stimulus (i.e PM2.5). During this study, for exam- 593 ple, wind direction was observed to explain 10% of the 594 variance of the TEOM monitor and the inclusion of this 595 parameter in the GBRT model improved results on ave- 596 rage by 5%. However, the affect of wind direction on 597 PM2.5 in this specific location may result from varia- 598 tions in the built environment that potentially include 599 PM sources (e.g buildings with specific boiler types), 600 which will likely differ from deployment locations. In- 601 cluding wind direction would therefore train the calibra- 602 tion model based on the specific conditions of the study 603 location instead of identifying the interaction of non-site 604 specific variables that affect the PPD42. Similarly, the 605 inclusion of a time-of-day parameter could led to erro- 606 neous calibration errors since diurnal PM2.5 trends may 607 be affected by local emission sources that vary per loca- 608 tion.

609 Furthermore, while a machine learning model can in- 610 crease overall performance, it is unable to explain mea- 611 surement error nor provide information about particle 612 properties. Feature importance is one method to un- 613 derstand how the model is using features to make pre- 614 dictions and adjust the sensor response, but it does not 615 necessarily describe the affect of certain meteorological 616 parameters, or combinations of parameters, on the sen- 617 sor's response.

618 4. Conclusion

619 This study demonstrates the suitability of a low-cost 620 aerosol monitor to measure intra-urban PM2.5 concen- 621 trations. Over a 47-day study period, three PPD42 sen- 622 sors, integrated with a Raspberry Pi microcontroller and 623 Bosch SHT31 temperature and relative humidity, were 624 deployed on the roof of an approximately 12m high 625 building proximate to a TEOM instrument installed and 626 operated by the NYS DEC. The devices were exposed

627 to wide variations in ambient temperature, relative hu-
 628 midity, barometric pressure, and precipitation in an en-
 629 vironment characterized by a diversity of urban land use
 630 types. Potential point sources of pollution included 56
 631 surrounding buildings using oil boilers for heating and
 632 the vehicular traffic along the Manhattan Bridge.

633 We evaluate three machine learning methods to cal-
 634 ibrate the deployed sensors, including traditional OLS
 635 regression, Ridge regression, and a GBRT decision tree
 636 model. Our results indicate that the GBRT model signif-
 637 icantly outperforms the OLS and Ridge models. Over-
 638 all, we find that low-cost aerosol devices can be used to
 639 inform community air quality monitoring efforts in het-
 640 erogeneous urban environments. The GBRT calibration
 641 method provides superior performance when combined
 642 with meteorological data that can be used to convert raw
 643 sensor readings to standard units. Importantly, this ma-
 644 chine learning approach can also be used to standardize
 645 readings across field-deployed sensors to improve rela-
 646 tive performance.

647 5. Acknowledgements

648 This research is supported in part by the UK Engi-
 649 neering and Physical Sciences Research Council (EP-
 650 SRC) Center for Doctoral Training in Urban Science
 651 and Progress (EP/L016400/1). We would like to thank
 652 the New York State Department of Environmental Con-
 653 servation for their assistance and expertise in conduct-
 654 ing the study. We would also like to thank the reviewers
 655 for their insightful comments and feedback.

656 6. References

- 657 Amaral, S. S., de Carvalho, J. A., Costa, M. A. M., and Pinheiro,
 658 C. (2015). An overview of particulate matter measurement instru-
 659 ments. *Atmosphere*, 6(9):1327–1345.
- 660 Austin, E., Novoselov, I., Seto, E., and Yost, M. G. (2015). Labora-
 661 tory evaluation of the shinyei pdp42ns low-cost particulate matter
 662 sensor. *PloS one*, 10(9):e0137789.
- 663 Castell, N., Dauge, F. R., Schneider, P., Vogt, M., Lerner, U., Fish-
 664 bain, B., Broday, D., and Bartonova, A. (2017). Can commercial
 665 low-cost sensor platforms contribute to air quality monitoring and
 666 exposure estimates? *Environment international*, 99:293–302.
- 667 Cheng, Z., Luo, L., Wang, S., Wang, Y., Sharma, S., Shimadera, H.,
 668 Wang, X., Bressi, M., de Miranda, R. M., Jiang, J., et al. (2016).
 669 Status and characteristics of ambient pm 2.5 pollution in global
 670 megacities. *Environment international*, 89:212–221.
- 671 Clougherty, J. E., Kheirbek, I., Eisl, H. M., Ross, Z., Pezeshki, G.,
 672 Gorczynski, J. E., Johnson, S., Markowitz, S., Kass, D., and Matte,
 673 T. (2013). Intra-urban spatial variability in wintertime street-level
 674 concentrations of multiple combustion-related air pollutants: the
 675 new york city community air survey (nyccas). *Journal of Exposure
 676 Science and Environmental Epidemiology*, 23(3):232.
- 677 De Vito, S., Esposito, E., Salvato, M., Popoola, O., Formisano, F.,
 678 Jones, R., and Di Francia, G. (2018). Calibrating chemical mul-
 679 tisensory devices for real world applications: An in-depth com-
 680 parison of quantitative machine learning approaches. *Sensors and
 681 Actuators B: Chemical*, 255:1191–1210.
- 682 Fishbain, B. and Moreno-Centeno, E. (2016). Self calibrated wireless
 683 distributed environmental sensory networks. *Scientific reports*, 6.
- 684 Friedman, J., Hastie, T., and Tibshirani, R. (2001). *The elements of
 685 statistical learning*, volume 1. Springer series in statistics New
 686 York.
- 687 Gao, M., Cao, J., and Seto, E. (2015). A distributed network of low-
 688 cost continuous reading sensors to measure spatiotemporal varia-
 689 tions of pm2. 5 in xi'an, china. *Environmental pollution*, 199:56–
 690 65.
- 691 Heimann, I., Bright, V., McLeod, M., Mead, M., Popoola, O., Stewart,
 692 G., and Jones, R. (2015). Source attribution of air pollution by
 693 spatial scale separation using high spatial density networks of low
 694 cost air quality sensors. *Atmospheric Environment*, 113:10–19.
- 695 Holstius, D. M., Pillarisetti, A., Smith, K., and Seto, E. (2014). Field
 696 calibrations of a low-cost aerosol sensor at a regulatory moni-
 697 toring site in california. *Atmospheric Measurement Techniques*,
 698 7(4):1121–1131.
- 699 Jerrett, M., Arain, A., Kanaroglou, P., Beckerman, B., Potoglou, D.,
 700 Sahsuvaroglu, T., Morrison, J., and Giovis, C. (2005). A re-
 701 view and evaluation of intraurban air pollution exposure models.
 702 *Journal of Exposure Science and Environmental Epidemiology*,
 703 15(2):185–204.
- 704 Jovašević-Stojanović, M., Bartonova, A., Topalović, D., Lazović, I.,
 705 Pokrić, B., and Ristovski, Z. (2015). On the use of small and
 706 cheaper sensors and devices for indicative citizen-based moni-
 707 toring of respirable particulate matter. *Environmental Pollution*,
 708 206:696–704.
- 709 Kaiser, H. and Specker, H. (1956). Bewertung und vergleich von
 710 analysenverfahren. *Fresenius' Journal of Analytical Chemistry*,
 711 149(1):46–66.
- 712 Kelly, K., Whitaker, J., Petty, A., Widmer, C., Dybwad, A., Sleeth,
 713 D., Martin, R., and Butterfield, A. (2017). Ambient and laboratory
 714 evaluation of a low-cost particulate matter sensor. *Environmental
 715 Pollution*, 221:491–500.
- 716 Kontokosta, C. E. (2016). The quantified community and neighbor-
 717 hood labs: A framework for computational urban science and civic
 718 technology innovation. *Journal of Urban Technology*, 23(4):67–
 719 84.
- 720 Kulkarni, P., Baron, P. A., and Willeke, K. (2011). *Aerosol mea-
 721 surement: principles, techniques, and applications*. John Wiley
 722 & Sons.
- 723 Kumar, P., Morawska, L., Martani, C., Biskos, G., Neophytou, M.,
 724 Di Sabatino, S., Bell, M., Norford, L., and Britter, R. (2015). The
 725 rise of low-cost sensing for managing air pollution in cities. *Envi-
 726 ronment international*, 75:199–205.
- 727 Manikonda, A., Žíková, N., Hopke, P. K., and Ferro, A. R. (2016).
 728 Laboratory assessment of low-cost pm monitors. *Journal of
 729 Aerosol Science*, 102:29–40.
- 730 Matte, T. D., Ross, Z., Kheirbek, I., Eisl, H., Johnson, S., Gorczyn-
 731 ski, J. E., Kass, D., Markowitz, S., Pezeshki, G., and Clougherty,
 732 J. E. (2013). Monitoring intraurban spatial patterns of multiple
 733 combustion air pollutants in new york city: design and implemen-
 734 tation. *Journal of Exposure Science and Environmental Epidemi-
 735 ology*, 23(3):223–231.
- 736 Mead, M., Popoola, O., Stewart, G., Landshoff, P., Calleja, M., Hayes,
 737 M., Baldovi, J., McLeod, M., Hodgson, T., Dicks, J., et al. (2013).
 738 The use of electrochemical sensors for monitoring urban air qual-
 739 ity in low-cost, high-density networks. *Atmospheric Environment*,
 740 70:186–203.
- 741 Molchanov, S., Levy, I., Etzion, Y., Lerner, U., Broday, D. M., and

- 742 Fishbain, B. (2015). On the feasibility of measuring urban air pol-
 743 lution by wireless distributed sensor networks. *Science of The Total
 744 Environment*, 502:537–547.
- 745 New York State Department of Transportation (2017). Traffic data
 746 viewer.
- 747 Pedregosa, F., Varoquaux, G., Gramfort, A., Michel, V., Thirion, B.,
 748 Grisel, O., Blondel, M., Prettenhofer, P., Weiss, R., Dubourg, V.,
 749 Vanderplas, J., Passos, A., Cournapeau, D., Brucher, M., Perrot,
 750 M., and Duchesnay, E. (2011). Scikit-learn: Machine learning in
 751 Python. *Journal of Machine Learning Research*, 12:2825–2830.
- 752 Pope III, C. A. and Dockery, D. W. (2006). Health effects of fine
 753 particulate air pollution: lines that connect. *Journal of the air &
 754 waste management association*, 56(6):709–742.
- 755 Schapire, R. E. (2003). The boosting approach to machine learning:
 756 An overview. In *Nonlinear estimation and classification*, pages
 757 149–171. Springer.
- 758 Shusterman, A. A., Teige, V. E., Turner, A. J., Newman, C., Kim,
 759 J., and Cohen, R. C. (2016). The berkeley atmospheric co 2 ob-
 760 servation network: initial evaluation. *Atmospheric Chemistry and
 761 Physics*, 16(21):13449–13463.
- 762 Snyder, E. G., Watkins, T. H., Solomon, P. A., Thoma, E. D.,
 763 Williams, R. W., Hagler, G. S., Shelow, D., Hindin, D. A., Ki-
 764 laru, V. J., and Preuss, P. W. (2013). The changing paradigm of air
 765 pollution monitoring.
- 766 Wang, Y., Li, J., Jing, H., Zhang, Q., Jiang, J., and Biswas, P. (2015).
 767 Laboratory evaluation and calibration of three low-cost particle
 768 sensors for particulate matter measurement. *Aerosol Science and
 769 Technology*, 49(11):1063–1077.

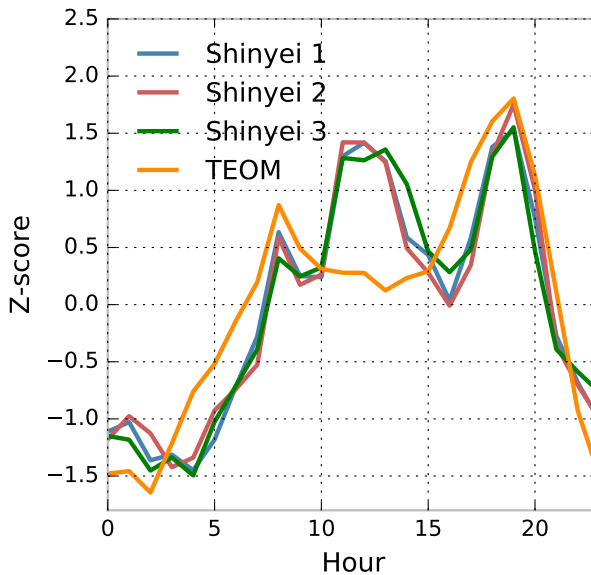


Figure S1: Average hourly measurements between three Shinyei PPD42 sensors and a TEOM reference instrument during a multi-week field calibration campaign. Z-scores are computed to compare uncalibrated sensor outputs and the reference instrument.

Table S1: Results of a sensitivity test to evaluate the relationship between meteorological conditions and the Shinyei PPD42 sensor response.

Parameter	R^2			
	Shinyei 1	Shinyei 2	Shinyei 3	TEOM
Temperature	0.25	0.24	0.30	0.15
Humidity	0.19	0.18	0.13	0.03
Dew Point	0.41	0.38	0.38	0.18
Sea Level Pressure	0.01	0.01	0.00	0.02
Wind Speed	0.10	0.11	0.09	0.10
Gust Speed	0.10	0.11	0.09	0.09
Wind Direction	0.12	0.11	0.12	0.02
Precipitation	0.00	0.00	0.00	0.00

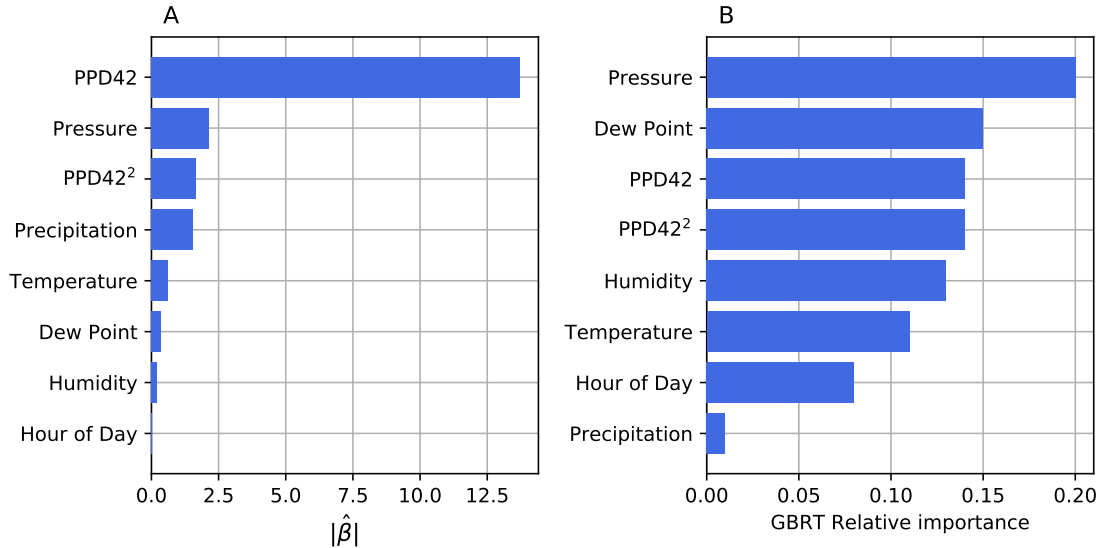


Figure S2: Feature importance for the ridge regression model (A) and the gradient boosting regression model(b).

Table S2: Multiple linear regression results for each PPD42 device based on test data. The target variable is the reference instrument (TEOM) and individual predictors are selected using best-subset selection.

Sensor	Model Summary		Explanatory Variable	Collinearity Analysis		
	R ²	BIC		β_1	p value	VIF
Shinyei 1	0.452	4729	β_0	8.18		6.76
			PPD42	4.46	0.000	
			Humidity	-1.11	0.000	
			Pressure	-0.71	0.000	
			PPD42 ²	-0.28	0.000	
			Temperature	-0.29	0.046	
Shinyei 2	0.507	4613	β_0	8.21		6.98
			PPD42	4.73	0.000	
			Humidity	-1.18	0.000	
			Pressure	-0.75	0.000	
			PPD42 ²	-0.31	0.000	
			Temperature	-0.30	0.009	
Shinyei 3	0.360	4924	β_0	7.96		4.75
			PPD42	3.31	0.000	
			Pressure	-0.86	0.000	
			Humidity	-0.56	0.000	
			Precipitation	-0.26	0.031	
			PPD42 ²	-0.09	0.210	

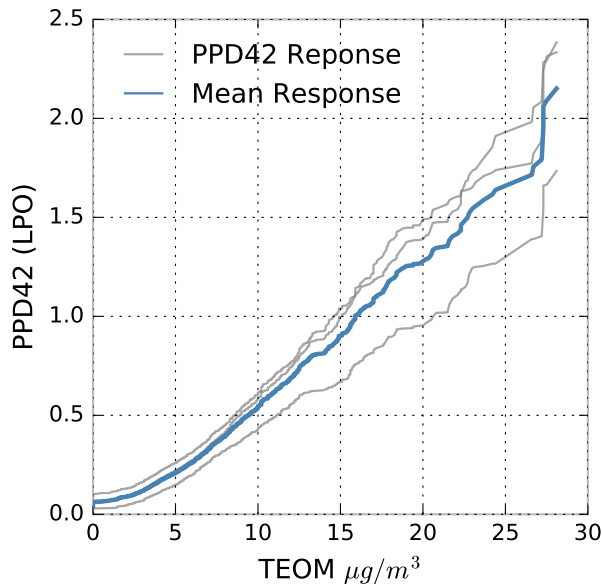
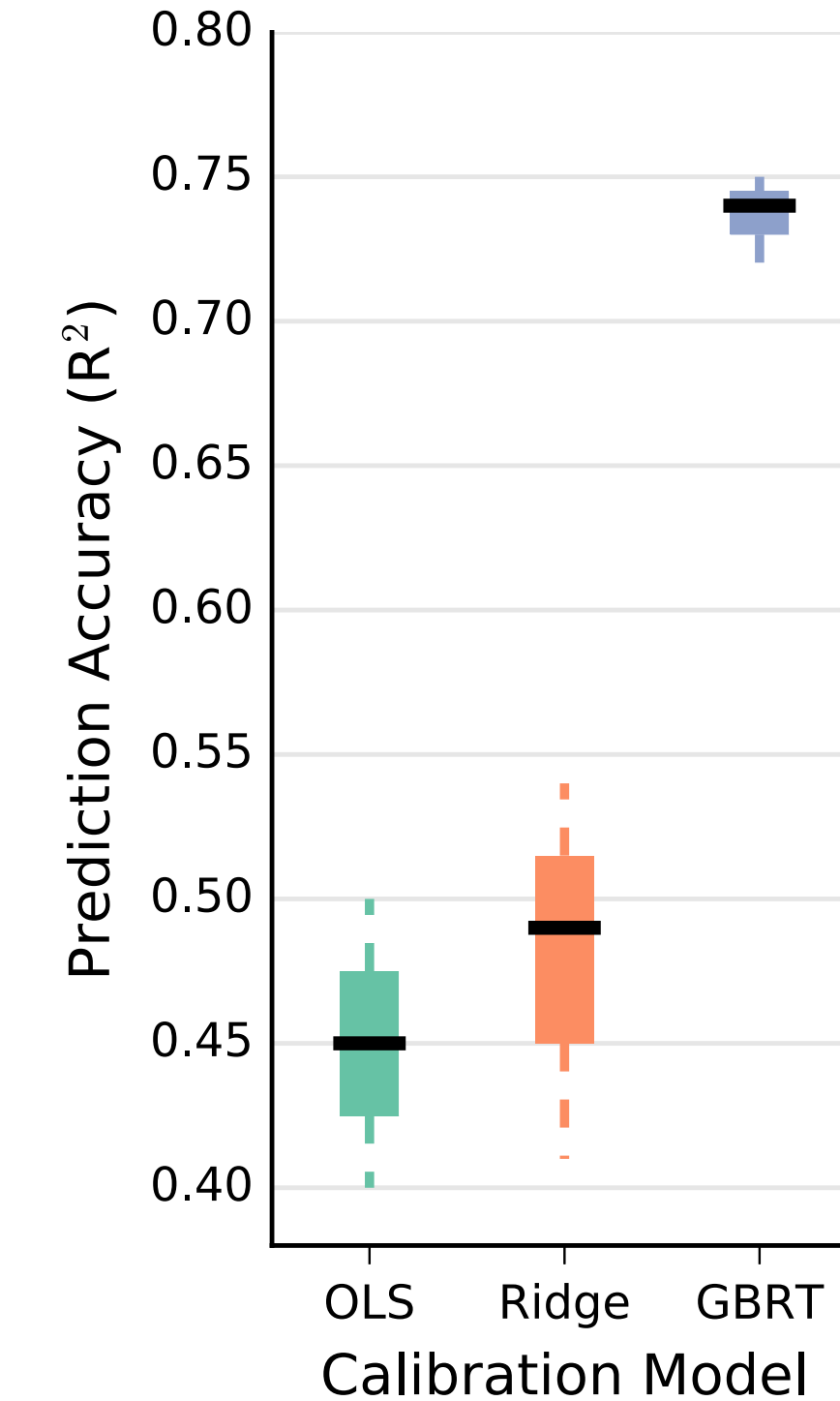
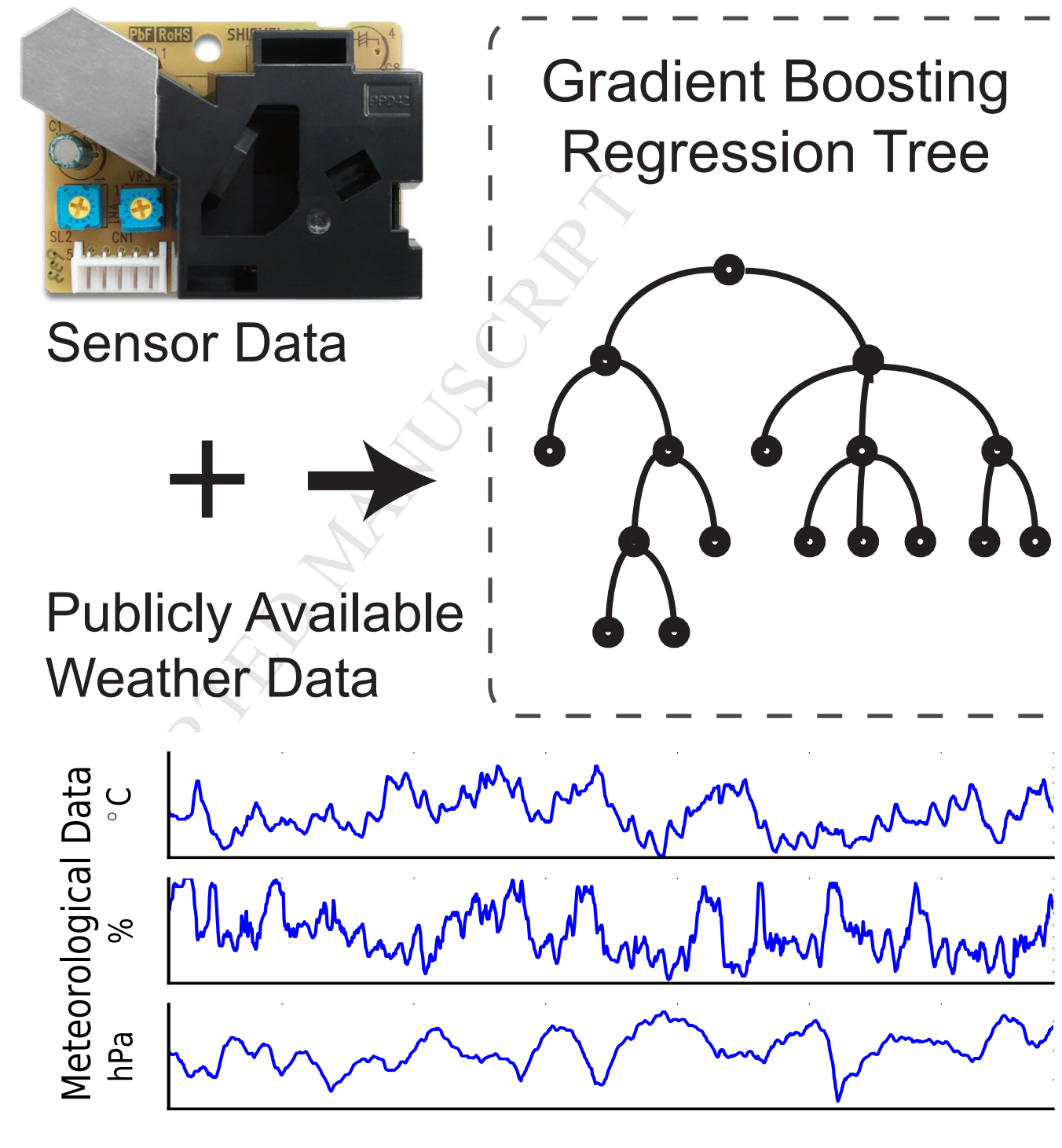


Figure S3: A comparison of individual PPD42 devices and their mean response with the TEOM reference instrument.

Table S3: Spatial characteristics surrounding the study location including land cover type and land use type.

{Data Type}	Class	50m	100m	250m	500m	1000m
Land cover	Tree canopy	5.85	7.99	5.16	12.96	11.88
	Grass/shrub	0.55	0.30	0.75	2.09	2.30
	Bare earth	0.0	0.0	0.0	0.25	0.10
	Water	0.0	0.0	0.0	0.0	12.83
	Buildings	42.05	30.69	36.63	36.27	30.87
	Roads	22.90	33.31	29.42	22.96	20.52
	Other paved surfaces	28.65	27.71	28.03	25.47	21.50
Total		100.0	100.0	100.0	100.0	100.0
Land Use	Commercial	2.03	7.42	9.53	7.12	10.93
	Industrial	9.06	4.90	3.70	2.20	2.18
	Mixed Residential & Commercial	3.88	7.09	19.75	28.21	22.69
	Open / Recreational Space	0.00	0.00	1.87	7.34	4.26
	Other	61.03	42.06	22.07	14.13	12.25
	Residential		0.00	2.83	5.54	10.00
	Vacant Land	6.59	12.92	4.77	1.29	1.75
Not Specified		17.41	25.61	35.48	34.17	35.92
Total		100.00	100.00	100.00	100.00	100.00
Boilers		0	0	1	6	56

Low-cost in situ PM_{2.5} monitoring



Highlights

- We calibrate low-cost air quality sensors in an urban environment in variable weather
- We improve calibration accuracy by using gradient boosting regression trees
- The design of our monitoring platform is a foundation for urban sensing networks
- The findings can enable reliable community air quality monitoring initiatives